**Title**: Evaluation of CMIP6 model performance against GHCND station observations across Asian cities

**Author(s), affiliation and email contact**: B. Goodsell, Earth System and Climate Centre, contact@climate.org.au

# Evaluation of CMIP6 model performance against GHCND station observations across Asian cities

B. Goodsell[1]

[1]Earth System and Climate Centre. ✉e-mail: contact@climate.org.au

Models from the Coupled Model Intercomparison Project (CMIP) are commonly used to infer future atmospheric temperatures across the world, including in Asia. This region is warming at an alarming rate, and home to some of the world's most populated countries and many of its most populated, fastest-growing and most heat-vulnerable cities. CMIP models are not always checked against local city-scale conditions without correction or downscaling applied beforehand. Being almost ten years after CMIP phase 6 was released, there is an opportunity to assess the accuracy of CMIP6 data with ground observations. Here we compare 2-metre air temperatures from 11 high-resolution CMIP6 models using a Shared Socioeconomic Pathway (SSP) for scenario 5-8.5 against GHCND station observations and ERA5 reanalysis for 411 Asian cities over the period 2015 to 2024. Neither bias correction nor downscaling was applied. ERA5 agreed closely with station observations ($r = 0.91$, RMSE = 2.2 °C), and all CMIP6 variants correlated significantly with observations but performed noticeably worse than reanalysis data ($r = 0.78$–$0.81$, RMSE = 4.17–5.35 °C, mean bias −1.26 to +3.28 °C). HadGEM3-GC31-HH performed best most often, and CNRM-CM6-1-HR performed worst. Biases were systematic rather than seasonal, with ten of the eleven variants being warm-biased in every season, and only CMCC-CM2-VHR4 being consistently cold. Performance depended strongly on geography, with latitude being the dominant predictor ($r = 0.84$). Agreement was strongest in arid, cold and temperate climates ($r \approx 0.88$–$0.91$) and weakest in tropical rainforest ($r = 0.23$) and monsoon ($r = 0.49$) climates. By region, Southeast Asian cities had the weakest agreement (mean $r = 0.43$) and East Asian cities the strongest ($r = 0.89$). The models were least reliable in tropical Southeast Asia, where heat-related mortality and urban growth are highest. Improving tropical convection and urban representation in models, and expanding observation networks, should be priorities for future model development.

## Introduction

As the global average air temperature continues to rise it is likely that the threshold of 1.5°C above pre-industrial temperatures will be breached within the next few years (Forster et al. 2025; World Meteorological Organization, 2025). Impacts to the environment and society, which are already being experienced by communities across the world (IPCC, 2021), will continue to worsen as and after this threshold is exceeded, with an increasing frequency of extreme weather events including heatwaves, floods, droughts, heavy precipitation and wildfires (United Nations, 2024). Beyond the impacts to the natural environment, increasing ambient air temperatures are also associated with increased levels of human impairment and injury as well as increased mortality rates (Basu & Samet, 2002; Flouris et al. 2018). Extreme heat is widely regarded as one of the most impactful extreme weather events with respect to human mortality, being responsible for an estimated 489,000 heat-related deaths every year between 2000 and 2019, with 45% of these located in Asia specifically (World Health Organization, 2024). In response to increasing air temperatures and the increasing frequency of heatwaves, many communities, particularly those in economically wealthy societies, have implemented adaptation measures, such as enhanced air conditioning, energy efficient buildings, cooling centers, and early warning systems (Pavanello et al 2021; Saffari et al. 2017; Meade et al. 2023; Lowe, Ebi & Forsberg 2011). However, given the limitations of human physiology, it is clear that even with widespread implementation of adaptation measures, the threat posed by extreme heat conditions will persist, meaning there is a need for targeted interventions in areas most at risk (World Health Organization, 2024).

Urban environments experience elevated temperatures and restricted airflow due to factors like heat absorption by concrete and asphalt, reduced greenery, air pollution, and heightened energy consumption, all of which contribute to the urban heat island (UHI) effect (Mohajerani et al., 2017). These and other factors contribute to high air temperatures in urban environments (Cheval et al 2024), with the fourth highest confirmed air temperature on record (inclusive of those measurements taken both within and outside of urban environments) being for the urban area of Turbat, Pakistan on 28 May 2017 reaching 53.7°C (± 0.4 °C; World Meteorological Organization, 2019). Surface temperatures in urban environment are capable of reaching upwards of 60°C (Mohajerani et al., 2017), and conventional paving materials such as asphalt can reach surface temperatures up to 152°F at mid-day (approximately 67°C; U.S. Environmental Protection Agency, 2025). While most urban environments experience varying levels of the heat island effect, some locations are notably cooler and more resilient than others due to factors including their latitude, climate zone, elevation, population, and urban planning approach, amongst other factors (Manoli et al 2019). Because of the variety of temperature responses in different urban environments, understanding the changing dynamics of heat waves, and their differences across regions is important for developing effective strategies to handle the negative impacts of climate change (IPCC, 2021).

Research into air temperatures across Asia in particular is important due to the fact that Asia: is warming at twice the global average (World Meteorological Organization 2025b); has the largest human population of all the continents and contains some of the most population dense cities in the world (United Nations 2024); has some of the fastest growing national populations and economies in the world (International Monetary Fund 2024); has some of the highest carbon emitting economies in the world (International Energy Agency 2025); and, has been experiencing record-breaking heatwaves that have had devastating impacts on human health, industry, and overall socio-economic stability (World Weather Attribution, 2024; United States Institute of Peace, 2024; Vu et al. 2025). The impact on communities in urban environments within Asia cannot be ignored, particularly given the region's extreme vulnerability to both climate change and rapid urbanization effects, and given the importance of Asian cities for industrial and economic activity that has direct impacts on the world (Shaw et al 2022; McKinsey Global Institute 2023). The impact of heat on urban environments in Asia has been broadly studied, including in East Asia where on average cities are 1.6–2.0°C warmer than their rural surroundings, and in Southeast Asian cities where average temperatures are up to 5.9°C warmer. Even within Asian cities, temperatures can be up to 7.0°C different between the coldest and warmest neighbourhoods due to the UHI effect (World Bank, 2023), and in Indian cities the UHI effect ranges between 2 and 10°C (Islam et al. 2024). Heat stress in urban Asian environments has been shown to result in productivity loses of 29-41% (Alahmad et al. 2025). Urban heat will become more impactful in the future, not just because of climate change, but also because of population movements. For example, in Southeast Asia in excess of 200 million more people are expected to relocate to cities by 2050 (Climate Impact Tracker, 2025), yet this region also experiences 45% of the world's heat-related deaths (World Health Organization, 2024). UHI impacts in tropical Asian cities are notably deadly, not just because heat-retaining surfaces such as concrete and asphalt enhance UHI and prevent proper cooling during nighttime, but also because of high humidity. This makes research into urban heat mitigation strategies increasingly important for protecting the hundreds of millions of Asian people moving to cities over the coming decades (Zhao et al., 2021).

Research on urban heat has been conducted in a variety of places within Asia, including: India, Bangladesh, Pakistan, Afghanistan, Sri Lanka, Nepal and Bhutan (Hassan et al. 2021; Maharjan et al. 2021; Kotharkar, Ramesh & Bagade 2018); China (Ren et al. 2008; Yang et al. 2025); Malaysia (Wang et al. 2019); Japan (Takane et al 2019); South Korea (Choi, Lee & Moon, 2018); the Philippines, Vietnam, Thailand and Indonesia (Nguyen et al. 2023); Singapore (Jung, 2024); Iran (Roshan, Sarli & Grab, 2021); Israel (Sofar and Potchter, 2006); Qatar, the UAE, Saudi Arabic, Oman, Kuwait and Bahrain (Abulibdeh 2021); and others (Tzyrkalli et al. 2024). There are variations in UHIs across Asia, which has resulted in spatial inequalities in heat exposure within individual cities (World Bank, 2023; Islam et al. 2024). Particularly in Asian cities, urban air pollution (Ulpiani 2021; Piracha & Chaudhary, 2022), high humidity environments (World Bank 2023), seasonal variation (Almeida et al. 2021; Yang et al., 2025), and differences between global North and South cities (Gao et al. 2024), are compounding factors to understanding this phenomenon.

### Comparing observational data with Earth system model outputs

Academic literature has also responded to the need for increased research on changes to Asian air temperatures by using computational climate models, including those produced by the ICCP and UN member states, to look at urban air temperatures in Asia. Such studies have often employed observational data for historical context alongside advanced climate projection models (e.g. the Coupled Model Intercomparison Project, CMIP) used to anticipate future conditions, while high-resolution data from meteorological reanalysis datasets like ERA5, MERRA-2, and NCEP are often used to provide broader coverage both spatially and temporally to analyze changes in air temperature during time periods where gaps in observational data exists (Eyring et al., 2016; Hersbach et al., 2020; Scafetta 2023). Such research provides insights into the current and future state of heat stress in the region and also informs adaptation and mitigation strategies to protect against escalating heat conditions (Turek-Hankins et al., 2021). CMIP models are typically compared to historical observations or reanalysis datasets (Papalexiou et al. 2020; Delgado-Torres et al 2022; Scafetta 2023), yet it is also important to make comparisons during the era of strongest change, and retrospectively comparing future model projections to observations provides a robust and independent test of model skill (Cowtan et al 2015; Hausfather et al 2020).

CMIP6 models have been an incredibly important tool in projecting future climate conditions, and have been used in numerous research studies, and also been important for informing government and policy decisions (IPCC 2021b). CMIP6 models have been used extensively for studying climate conditions in Asia (Supharatid et al 2022; Mousavikhaledi et al 2025; Zhang, Wu & Zhao 2025), including for various Asian cities (Bhanage et al 2023; Goyal et al 2023; Bhanage et al. 2024), and have also been evaluated for their performance in Asia (Luo et al 2020; Yang et al 2021; Hamed et al 2022; Wenqiang et al 2022; Azad & Ahmadi 2024). Because of their widespread use, it is important that they're validated against observational data, which is important, not only for enhancing model accuracy but also for strengthening public trust in climate projections. Although these models, known categorically as global circulation models (GCMs), are typically used and validated at broader geospatial scales, such validation should be also undertaken at local scales of tens of kilometres where climate impacts are most acutely experienced by ecosystems and communities (Seneviratne et al., 2021; Reyes-Garcia et al 2024), and in vulnerable regions such as Asia, where heat stress poses socioeconomic and health challenges (Watts et al., 2021).

Evaluation of CMIP6 model performance for temperature simulations have already been undertaken across various spatial and temporal scales revealing both model strengths and weaknesses (Craigmile & Guttorp, 2023; Zhang et al., 2023). This includes for particular regions within Asia, such as studies on the Tibetan Plateau, which demonstrated some improvements in CMIP6 compared to earlier CMIP5 models, but also some areas where model results have changed very little (Zhu & Yang 2020; Lalande et al 2021; Cui, Li & Tian 2021). CMIP6 model performance across arid regions of Northwest China have revealed systematic biases and it has been recommended to use optimal model combinations for specific regional applications (Liu et al., 2022). The evaluation of multi-model ensembles has identified both model capabilities and limitations in reproducing observed extreme temperature patterns in Asia (Kim et al., 2020). Because of limitations in these models, bias correction techniques for CMIP6 temperature projections have evolved for various applications and regional contexts (Jose & Dwarakish 2022; Lafferty & Sriver 2023; Li & Li 2023; Kong & Huber 2024; Singh et al 2024). Dynamical downscaling applications are often used for high-resolution applications (Xu et al., 2021; Try & Qin 2024), and high-resolution global datasets derived from statistically and AI downscaled CMIP6 models have been created for urban and regional applications (Kumar et al., 2024; Pan et al., 2024; Yuan et al 2024). Because GCMs are often produced at a broader geospatial resolution and unable to capture high-resolution behaviour, it is typically and reasonably assumed that such models are not accurate for looking at high-resolution climate conditions (Rampal et al. 2024). Because of this, comparisons to high-resolution observational data is typically not undertaken without downscaling or bias correction efforts first (e.g. Kong & Huber 2024; Kumar et al., 2024; Pan et al., 2024; Singh et al 2024; Try & Qin 2024; Yuan et al 2024). However, these processes can introduce additional uncertainties and computational demands that constrain widespread practical application (Lafferty & Sriver 2023).

As the CMIP6 climate projection dataset approaches its tenth anniversary since its release in 2016 (Eyring et al., 2016), the scientific community has an opportunity for evaluating the reliability of these climate models against empirical observations over an entire decade's worth of data. Such longer-term comparison and evaluation of CMIP6 performance should be considered more reliable than shorter-term comparisons (Delgado-Torres et al 2022). Because of these factors there is validity in assessing the bias of CMIP6 models in predicting surface air temperatures in urban environments in Asia with comparison to datasets over the past decade, such as reanalysis datasets and detailed ground observations. The Global Historical Climatology Network-Daily (GHCND) dataset is one such detailed ground observation dataset, comprised of more than 100,000 weather stations worldwide with records spanning decades to over a century (Lawrimore et al., 2011; Menne et al., 2012). While most stations only capture temperature records, this dataset's large temporal and spatial coverage makes it an important resource for evaluating CMIP6 model performance (Perkins-Kirkpatrick & Lewis, 2020; Hirsch et al 2021), and given its reputable status as a comprehensive dataset, allows researchers to identify systematic biases and improve future CMIP model iterations (Zhong et al 2022; Gebrechorkos et al. 2023).

The comparison of CMIP6 projections with GHCND observations could potentially bridge the gap between global climate modelling and regional impact assessments, enabling more targeted interventions for understanding of air temperature changes and heat stress mitigation (Maraun & Widmann, 2018). This comparative analysis would be particularly useful in regions characterised by complex topography, diverse land use patterns, or unique meteorological conditions that may not be fully resolved in global climate models with horizontal resolutions of 50-200 kilometres (Rummukainen, 2010). Such validation exercises done over a longer-term (decade or longer) could further enhance statistical downscaling techniques and bias correction methods that enhance the application of CMIP6 outputs for local decision-making processes in the urban environment (Yiou et al. 2024). Because of this, the evaluation of CMIP6 models against GHCND observations and reanalysis products in urban areas across Asia represent an important step toward developing more robust early warning systems for heat waves and implementing effective adaptation measures in heat-vulnerable sectors (Lowe et al., 2018). By identifying where models have good or poor agreement with observed temperatures, researchers can provide more refined guidance on the likelihood and severity of future heat stress conditions under various emissions scenarios (Hawkins & Sutton, 2009). This information is important for prioritising interventions in regions where the combination of climatic and socioeconomic factors creates particularly high vulnerability to heat-related impacts (Hoegh-Guldberg et al., 2018).

## Method

This analysis relies on the European Centre for Medium-Range Weather Forecasts Reanalysis v5 (ERA5), the Coupled Model Intercomparison Project Phase 6 (CMIP6), and the Global Historical Climatology Network Daily (GHCND) station observations, and evaluates CMIP6 model outputs against observational records and reanalysis products at local scales across Asia during the decade spanning 2015-2024. Urban areas within Asia were selected based on three conditions, some of which were overlapping: cities with a population exceeding 750,000 inhabitants (n=429, population data sourced from the GeonamesCache library https://github.com/yaph/geonamescache), national capital cities (n=49), and the two most populous urban areas within each nation (n=98). While this resulted in 508 cities being selected, many were subsequently excluded based on data coverage and availability.

GHCND meteorological stations were matched with a given city using a one-degree grid cell centered on each city's latitude and longitude coordinates. Temporal filtering excluded stations that lacked coverage at any time during the January 1940 to December 2024 period, with the 1940 year chosen to align with the start date of ERA5 dataset, and 2024 being chosen as 10 years since the beginning of the CMIP6 dataset. From an initial pool of 2,407 stations within the defined spatial boundaries of the 508 cities, only 1,731 stations met the temporal coverage criteria. While analysis was initially considered to include precipitation, wind speed, and humidity measurements, many stations lacked this data, with only temperature records being available. Despite limiting the analysis to temperature data only, the availability and coverage of observational records meant that the final analysis was done with respect to 411 cities, rather than 508. Daily temperature averages were computed from GHCND records, and where multiple stations geospatially matched with any given city, a simple mean average of these station values was taken if and when temporal overlap also occurred.

ERA5 2-meter air temperature data was accessed through the Climate Data Store Application Program Interface (CDSAPI) for the period January 1940 to December 2024. Hourly temperature fields were extracted at each cities coordinates and temporally averaged to daily values. CMIP6 model selection was based on datasets that had sufficient spatial and temporal resolution characteristics, primarily that they offered data on a daily or sub-daily temporal resolution and a sub-100 kilometre spatial resolution, and were available from data repositories at the time of analysis. SSP585 data was chosen to represents a high-emissions climate scenario. The following models were covered by the analysis using data either provided in daily averages or a daily average was calculated from subdaily data:

- CMCC-CM2-VHR4-r1p1i1f1
- CNRM-CM6-1-HR-r1i1p1f2
- EC-Earth3P-HR variants: r1i1p2f1, r2i1p2f1, r3i1p2f1
- EC-Earth3P-r3i1p2f
- HadGEM3-GC31 variants: HH-r1i1p1f1, HM-r1i1p1f1, HM-r1i2p1f1, HM-r1i3p1f1
- MPI-ESM1-2-XR-r1i1p1f1

Each city was characterized using multiple environmental factors: climate classifications followed the Köppen-Geiger system (https://doi.org/10.1038/s41597-023-02549-6), while ecological context was determined based on terrestrial ecoregion mapping (https://academic.oup.com/bioscience/article/67/6/534/3102935; https://ecoregions.appspot.com/). The most represented Koppen-Geiger climate zones were Temperate_no_dry_hot (93), Temperate_dry_winter_hot (76), and Tropical_savannah (45), while the least represented were Cold_no_dry_hot, Cold_dry_winter_cold, and Temperate_no_dry_warm (1 city each). Urban characteristics were based on Local Climate Zones (https://zenodo.org/records/6364594) while topographic information was obtained via the Open Elevation API (https://api.open-elevation.com/). The most represented Local Climate Zones were Compact_mid-rise (116), Compact_low-rise (98) and Large_low-rise (72), while the least represented were Bare_soil_sand and Lightweight_low-rise (1 city each). See Appendix 1 for more details of the number of cities per climate category.

Statistical validation used standard meteorological verification metrics including Pearson correlation coefficients, mean absolute differences, root mean square error (RMSE), the Willmott skill score, quantile-quantile regression slopes, and seasonal bias assessments. Performance evaluation was undertaken by producing statistical measures for each model variant and also with respect to each environmental classification systems (Köppen-Geiger zones, terrestrial ecoregions, local climate zones, and elevation bands) to identify associations between model performance and environmental characteristics. Ranking analyses quantified individual model performance across different classification schemes and statistical measures. Multiple regression modeling was subsequently employed to identify environmental predictors (including latitude, longitude, elevation, population, local climate zone, Köppen climate zone, biome, biome realm, and model) most strongly associated with model performance across different statistical measures. Neither bias correction nor statistical downscaling was applied to the model outputs, to ensure direct comparison of raw model data against the observational record.

## Results

Comparison between ERA5 reanalysis data and GHCND station observations revealed strong agreement, with a Pearson correlation coefficient of $r = 0.91$ (95% CI: 0.89–0.92, $p < 0.001$). The analysis yielded a root-mean-square error of 2.2°C, a mean bias of 0.98°C, and a skill score of 0.89. All 11 CMIP6 model variants showed lower correlations compared to ERA5 when validated against GHCND observations, however, despite this, all model variants showed significant correlations with observations ($p < 0.001$). Model correlations with observations ranged from 0.78 to 0.81 (mean = 0.79), while mean differences ranged from -1.26°C to 3.28°C (mean 1.37°C), and root-mean-squared-error values ranged from 4.17°C to 5.35°C (mean = 4.44°C). HadGEM3-GC31-HH-r1i1p1f1 emerged as the best-performing model variant overall with the highest correlation ($r = 0.81$, 95% CI: 0.78–0.83, $p < 0.001$) and lowest RMSE (4.17°C), while CMCC-CM2-VHR4-r1p1i1f1 and CNRM-CM6-1-HR-r1i1p1f2 showed the poorest performance with the lowest correlation ($r = 0.78$) and the highest root-mean-squared-error values (4.78°C and 5.35°C, respectively), while also exhibiting the largest negative and positive biases (-1.26°C and 3.28°C, respectively).

**Table 1 |** Summary verification statistics for GHCND station observations against ERA5 reanalysis and each CMIP6 model variant. Each row compares GHCND with the named product; columns give the Pearson correlation coefficient, mean difference, root-mean-square error, quantile–quantile regression slope and the number of paired daily values contributing to each comparison.

| comparison | correlation | mean_diff | rmse | qq_slope | count |
|---|---|---|---|---|---|
| CMCC-CM2-VHR4-r1p1i1f1 | 0.781 | -1.26 | 4.777 | 1.106 | 3,219 |
| CNRM-CM6-1-HR-r1i1p1f2 | 0.776 | 3.276 | 5.351 | 1.095 | 3,221 |
| EC-Earth3P-HR-r1i1p2f1 | 0.792 | 1.77 | 4.347 | 1.054 | 3,221 |
| EC-Earth3P-HR-r2i1p2f1 | 0.793 | 1.645 | 4.331 | 1.066 | 3,221 |
| EC-Earth3P-HR-r3i1p2f1 | 0.794 | 1.527 | 4.225 | 1.046 | 3,221 |
| EC-Earth3P-r3i1p2f1 | 0.79 | 1.123 | 4.199 | 1.08 | 3,221 |
| ERA5 | 0.907 | 0.991 | 2.3 | 0.933 | 15,551 |
| HadGEM3-GC31-HH-r1i1p1f1 | 0.806 | 1.319 | 4.169 | 1.08 | 3,160 |
| HadGEM3-GC31-HM-r1i1p1f1 | 0.794 | 1.591 | 4.395 | 1.097 | 3,160 |
| HadGEM3-GC31-HM-r1i2p1f1 | 0.798 | 1.723 | 4.381 | 1.083 | 3,160 |
| HadGEM3-GC31-HM-r1i3p1f1 | 0.795 | 1.367 | 4.271 | 1.076 | 3,160 |
| MPI-ESM1-2-XR-r1i1p1f1 | 0.786 | 0.934 | 4.394 | 1.152 | 3,221 |

### Seasonal Bias

Seasonal bias patterns revealed distinct differences across CMIP6 models. Ten of the eleven model variants exhibited consistent positive bias across all seasons, while only CMCC-CM2-VHR4-r1p1i1f1 showed consistent negative bias throughout the year. No models demonstrated mixed seasonal bias patterns, suggesting that temperature biases in CMIP6 models are largely systematic rather than seasonally variable.

Among models with positive bias, CNRM-CM6-1-HR-r1i1p1f2 showed the largest warm bias with values ranging from 2.52°C in summer to

4.03°C in winter. HadGEM3 model variants displayed the smallest positive biases among the warm-biased models, particularly during summer (0.25-0.61°C). MPI-ESM1-2-XR-r1i1p1f1 showed the most balanced seasonal performance among positive-biased models, with biases ranging from only 0.10°C in summer to 1.74°C in winter. CMCC-CM2-VHR4-r1p1i1f1 was the only model that was consistently cold across all seasons, ranging from -0.37°C during winter to -2.22°C during summer.

### Performance by Physical Characteristics

Model performance varied across different Köppen climate zones, with cities in arid, cold, temperate and tropical savannah regions performing well. By correlation, those located in Cold dry winter hot climates showed the best performance ($r = 0.91$, $n = 42$), followed by all arid classifications (Arid desert hot: $r = 0.90$, $n = 23$; Arid steppe/desert cold: $r = 0.89$, with $n = 33$ and $n = 6$, respectively; and Arid steppe hot: $r = 0.88$, $n = 26$). Whilst the worst performance occurred in Tropical rainforest ($r = 0.23$, $n = 22$), and Tropical monsoon areas ($r = 0.49$, $n = 23$), Tropical zones had the lowest RMSE (2.0 to 2.9°C, Tropical savannah $n = 45$), while those located in Cold no dry hot zones had the largest RMSE (8.5°C, $n = 1$), which also had the largest mean difference (4.5°C), while Temperate dry winter warm zones had the smallest mean difference (-0.2°C, $n = 4$).

By correlation, cities located in biomes classified as Temperate Conifer Forests ($n = 4$) showed the highest model to observation correlations ($r = 0.91$), followed by Temperate Broadleaf & Mixed Forests ($r = 0.89$, $n = 147$) and Montane Grasslands & Shrublands ($r = 0.89$, $n = 2$). While cities located in Tropical biomes consistently showed the poorest performance, with Tropical & Subtropical Moist Broadleaf Forests exhibiting the lowest correlations ($r = 0.64$, $n = 127$), they also showed some of the lowest RMSE values, with Mangroves having the lowest RMSE value (2.8°C, $n = 4$). Comparatively, grasslands showed the highest RMSE values, with Montane Grasslands & Shrublands being the highest (6.8°C, $n = 2$). Grasslands also had some of the largest mean differences, with Tropical & Subtropical Grasslands, Savannas & Shrublands having the highest (4.7°C, $n = 2$), while Temperate Conifer Forests had the lowest (0.8°C, $n = 4$).

By biome realms, Palearctic, Afrotropic and Indomalayan areas had good correlation ($r = 0.89$, $n = 214$; $r = 0.88$, $n = 4$; and $r = 0.70$, $n = 176$, respectively), while a single Australasian city had poor correlation ($r = 0.12$, $n = 1$), however this was different for RMSE values, with the Australasian city having the lowest RMSE values (2.3°C), and Afrotropic cities having the highest RMSE values (5.4°C). Afrtropic cities also had the highest mean difference (4.7°C), while Indomalayan cities had the lowest mean differences (1.2°C).

Analysis of cities by Local Climate Zone (LCZ) showed that the city located in areas classified as Bare soil/sand had the highest correlations ($r = 0.92$ $n = 1$), while Open low-rise urban areas performed worst ($r = 0.62$, $n = 37$). However, by RMSE value and mean difference Open low-rise areas performed best (3.6°C and 0.8°C, respectively), while the city located in Lightweight low rise areas performed the worse (7.1°C and 3.2°C, respectively, $n = 1$).

Correlation did not vary substantially by population, with cities classified as Very Small (3.8 million persons or lower; $r = 0.78$, $n = 360$) similar to the single city classified as Very Large (19.0 million; $r = 0.84$, $n = 1$). Correlations varied somewhat by elevation with those classified as being at Very Low elevations (under 439 metres; $r = 0.77$, $n = 327$) performing worse than those classified as being at High elevations (1357 metres to 1816 metres; $r = 0.91$, $n = 10$), however model performance dropped above this elevation (Very High; $r = 0.82$, $n = 6$).

When comparing model performance to GCHND observations across all Asian cities by different combinations of climate zone (Koppen, LCZ, REALM, BIOME) and metric (correlation, rmse, mean difference, and seasonal biases), HadGEM3-GC31-HH-r1i1p1f1 performed best most often, while CNRM-CM6-1-HR-r1i1p1f2 performed worst most often.

### Feature importance and predicting model performance

Analysis of performance metric relationships with physical variables showed that latitude was the dominant predictor of model performance, showing very strong positive correlations with model-observation correlation coefficients ($r = 0.84$, $p < 0.001$) and RMSE values ($r = 0.64$, $p < 0.001$). This indicates that models performed progressively better at higher latitudes across Asia, with the poorest performance in tropical and subtropical regions.

Regression analysis revealed that CMIP6 model performance can be predicted with high accuracy using geographic and environmental variables. Model-observation correlation emerged as the most predictable performance metric ($R^2 = 0.94$, RMSE = 0.06), while seasonal biases were least predictable ($R^2 = 0.29$-$0.44$).

Cross-validation results indicated good model stability for correlation prediction (CV $R^2 = 0.772 \pm 0.168$) and RMSE prediction (CV $R^2 = 0.667 \pm 0.118$), but showed higher uncertainty for seasonal bias predictions (CV $R^2$ ranging from 0.073-0.598). The dataset was reasonably sized with 1,760 training samples and 759 test samples.

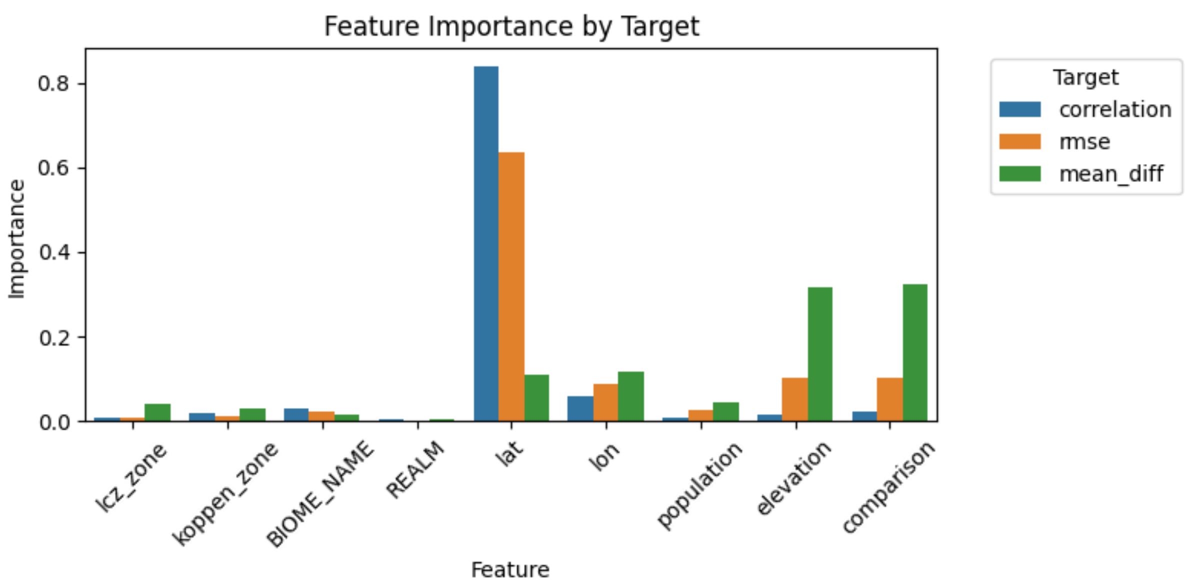


**Fig. 1 |** Relative importance of geographic and environmental predictors of CMIP6 model performance. Importance is shown separately for three performance targets — model–observation correlation, RMSE and mean difference — across Local Climate Zone, Köppen–Geiger zone, biome, biogeographic realm, latitude, longitude, population, elevation and model comparison.

### Consideration to political geography

Cities located in South-Eastern Asia (n = 49) had the poorest correlation between observations recorded in the GHCND dataset and modelled predictions from CMIP6 outputs (m=0.43, range=0.38 to 0.50), whilst those cities located in Eastern Asia (n = 208) had the highest correlation (m=0.89, range=0.84 to 0.92), although this correlation value was not overly dissimilar to that for cities located in Central Asia (m=0.85, n = 8) or Western Asia (m=0.89, n = 49), while cities from Southern Asia had slightly poorer correlation (m = m=0.79, range=0.70 to 0.83, n = 97). The mean difference between GHCND observations and CMIP6 predictions were lowest for cities in Central Asia (m=0.14, range=-0.61 to 0.88), and highest for those cities located in Eastern Asia (m=1.84, range =0.86 to 3.06). Central Asia, though poorly represented by the number of cities in the analysis, was the only region where cities experienced consistent cold bias during summer or autumn in model predictions compared to observations (m = -1.09, range=-0.32 to -1.86; and m = -1.57, range=-0.89 to -2.25), while cities in all regions typically experienced warm biases in model outputs.

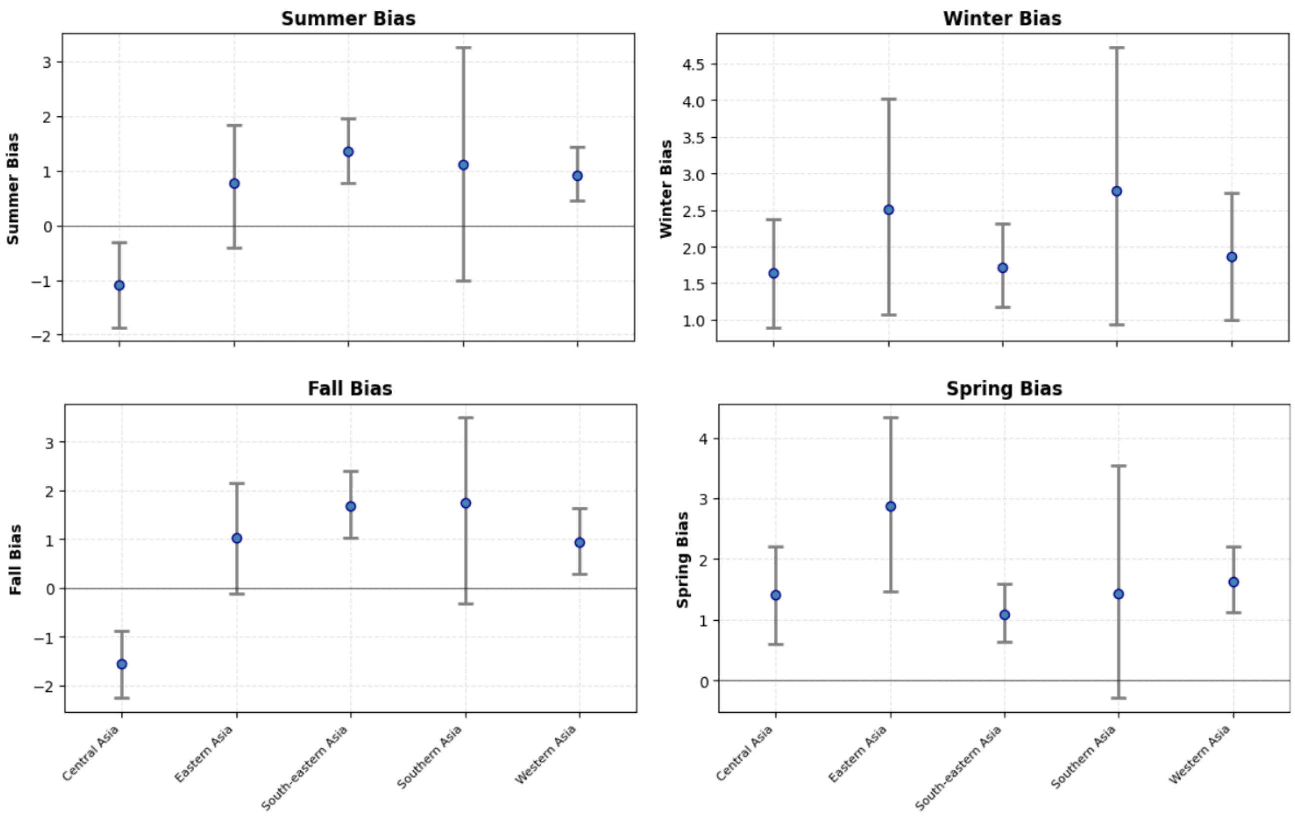


**Fig. 2 |** Seasonal temperature bias by Asian subregion. Top row, summer and winter; bottom row, autumn and spring. Points give the mean bias across cities in each United Nations geographic subregion and bars span the range across model variants; all panels share the subregion categories labelled on the bottom row.

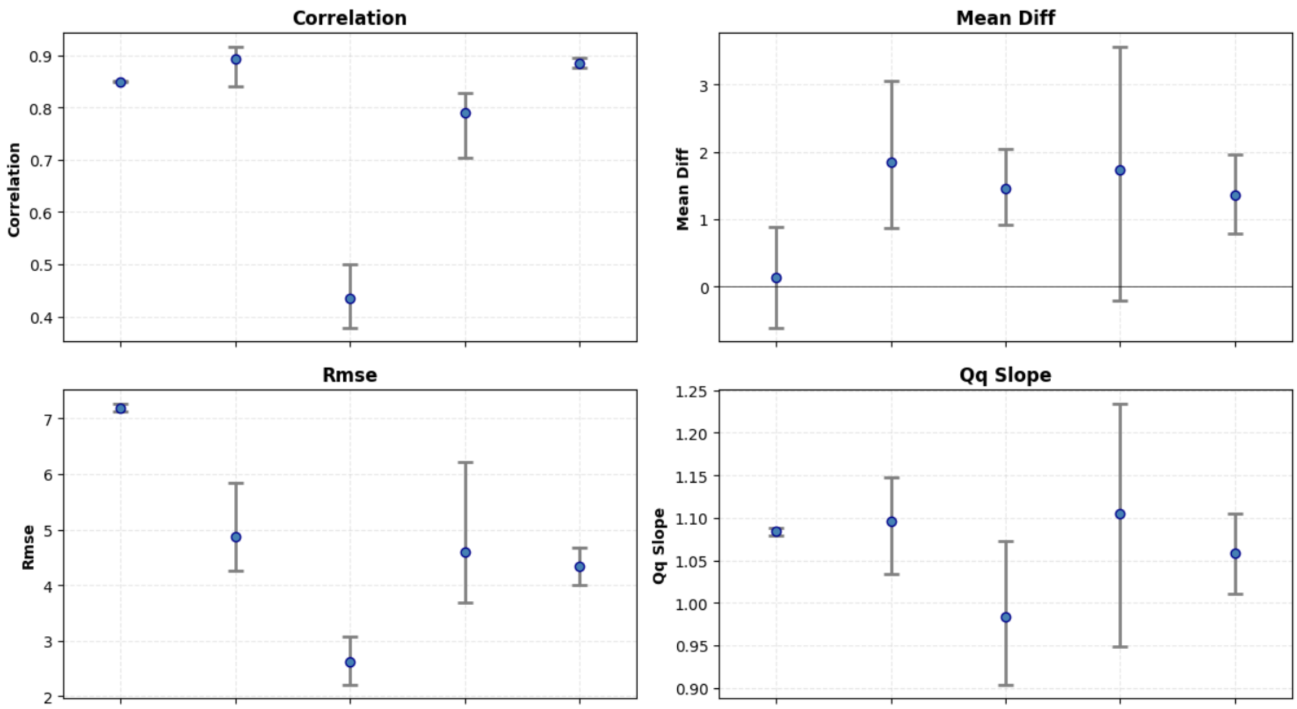


**Fig. 3 |** Model–observation performance metrics by Asian subregion. Correlation, mean difference, RMSE and quantile–quantile slope; x-axis category labels are absent from the source image.

## Discussion

The analysis of CMIP6 performance compared to GHCND observations for Asian cities shows that even though CMIP6 models represent a substantial advancement in global climate modelling capabilities, their application to urban-scale temperature assessment in Asia requires careful correction for different geographic, climatic, and urban morphological factors. Results show that ERA5 reanalysis is strongly correlated with GHCND observations (r=0.91), and overperforms when compared to CMIP6 models (r=0.776-0.806, RMSE 4.17-5.35°C). This performance gap is consistent with previous studies examining CMIP6 model evaluation in Asia (Almazroui et al., 2020; Gusain et al., 2020), though our analysis provides more comprehensive spatial coverage across urban centers. The systematic nature of these biases, with ten of eleven models showing consistent positive bias across all seasons, suggests fundamental limitations in model physics rather than regional calibration issues. Of course, this performance gap reflects the inherent limitations of CMIP6's coarse spatial resolution (typically 50-200 kilometres), which cannot adequately capture the complex thermal dynamics and spatial heterogeneity characteristic of urban heat islands and fine-scale physical behaviours, for which regional and local scale models are more appropriate. HadGEM3-GC31-HH-r1i1p1f1 consistently performed best across different measures and climate zones. This aligns with previous evaluations of the HadGEM3 model family, which has shown superior performance in representing Asian climate patterns (Rostron et al., 2020). The HadGEM3 models' dominance in four of the top five performance positions suggests that the Met Office's model development priorities, particularly their focus on tropical convection schemes and monsoon representation, have yielded measurable improvements in Asian climate simulation (Williams et al., 2018).

There was an elevation-dependent performance patterns, with optimal correlations around 2000m elevation, potentially reflecting where models may better represent large-scale temperature advection compared to surface-atmosphere interactions (Pepin et al., 2015). However, the decline in performance at very high elevations suggests that snow-albedo feedbacks and complex topographic effects may also be impactful on model performance. There was a strong latitudinal gradient in model performance, with latitude explaining 84% of variance in model-observation correlations. The deterioration in model performance from temperate to tropical regions, ranging from 0.229 in tropical rainforest climates to 0.918 in bare soil/sand environments, more generally has also been noted in other CMIP evaluations (Tapiador et al., 2019; Eyring et al., 2020). The poor performance in tropical rainforest (Köppen Af) and monsoon (Am) climates suggests that current convection parameterizations inadequately capture the diurnal cycle of tropical convection and its interaction with large-scale circulation patterns (Dai, 2006; Kooperman et al., 2018). By climate zone, arid and semi-arid regions performed well (r > 0.88 for most desert classifications) likely reflecting locations where latent heat flux uncertainties are minimized (Mueller & Seneviratne, 2012), temperature forests and cold climates also performed well, with poor performance in tropical moist forests (r = 0.641) and mangroves (r = 0.734) likely reflect complex thermal interactions which remain challenging for global climate models (Mauritsen & Stevens, 2015; Sherwood et al., 2020). This poor performance in tropical regions is a substantial concern given these areas are home to some of Asia's most populous and rapidly urbanizing cities. Southeast Asia currently accounts for 45% of global heat-related deaths and is projected to be among the worst-hit regions in terms of heat-related mortality under all adaptation scenarios. They also experience substantial economic losses during extreme heat events. With over 200 million additional people expected to move to Southeast Asian cities by 2050, this geographic mismatch represents an important gap in climate science capacity to support informed decision-making in a region that is experiencing rapid climate change (Hijioka et al., 2014). Other evaluations of CMIP6 models across Southeast Asia have similarly demonstrated mixed performance (Hamed et al., 2022; Desmet & Ngo-Duc, 2021).

The better performance for bare soil/sand LCZ areas (r = 0.92) compared to open low-rise urban areas (r = 0.62) suggests that model errors are amplified in environments with complex built structures and heterogeneous land cover. This pattern reflects the inability of coarse-resolution models to represent the three-dimensional urban canopy structure, anthropogenic heat fluxes, and modified surface energy balance that characterize urban environments. Advanced downscaling techniques, such as the deep learning-based 0.1° resolution CMIP6 datasets developed for East Asia, show promise for addressing these limitations by providing spatial detail suitable for urban-scale applications, though their performance still requires validation against urban observation networks. Compact high-rise zones (r = 0.879) outperformed open high-rise zones (r = 0.752), suggesting that CMIP6 models may better represent the thermal properties of dense urban environments, possibly due to the averaging effects of urban heat island intensity over grid cells (Zhao et al., 2014). However, the relatively small sample sizes in some urban categories limit the reliability of these findings. Variation in optimal model performance across different physical characteristics (Köppen zones, biomes, Local Climate Zones) indicates that no single model provides superior performance. This finding aligns with recent research on CMIP6 model evaluation, which has demonstrated that individual GCMs exhibit varying performance rankings for different extreme precipitation indices, and that model selection can significantly impact evaluation results.

A majority of model variants experienced positive temperature across seasons (only CMCC-CM2-VHR4 showed consistent negative bias) indicating systematic issues with surface energy balance representation. Warm biases in climate models are commonly attributed to insufficient cloud cover, particularly in tropical regions where convective cloud parameterizations may underestimate cloud fraction (Vial et al., 2013; Zelinka et al., 2020). These biases have substantial implications for heat-health impact assessments, as recent research demonstrates that even modest temperature increases translate directly to mortality risk—with studies showing a 2% increase in non-accidental deaths per 1°C increase in temperature above optimal values across Asian cities (Cheng et al., 2024). Given that urban heat islands already contribute to elevated mortality rates in major Asian metropolitan centers, with over 100,000 annual heat-related deaths in the East Asia and Pacific region, systematic warm biases in climate projections could lead to substantial underestimation or overestimation of adaptation needs depending on model selection.

Results demonstrate that basic geographic coordinates including latitude and elevation can predict CMIP6 model performance with moderate accuracy, suggesting that systematic model deficiencies are primarily related to physical processes such as tropical convection and monsoon dynamics, rather than local-scale heterogeneity. This could improve ensemble construction by weighting models based on their expected performance in particular geographic domains (Sanderson et al., 2015). Thus, model evaluation focusing on factors such as tropical convection, monsoon dynamics, and land-atmosphere interactions should be prioritised in future CMIP development cycles. The systematic nature of these biases across all models examined indicates that the issues are not model-specific but rather reflect common limitations in representing fundamental physical processes. This predictive capability could enable more informed model selection and uncertainty quantification for Asian cities lacking comprehensive observational networks. However, the lower predictability of seasonal biases ($R^2$ = 0.29-0.44) indicates that temporal accuracy remains more challenging to forecast, limiting the reliability of seasonal adaptation planning based on model projections alone.

From a regional perspective, the geographic imbalances in model performance across political boundaries have important policy implications. The relatively strong performance in Eastern Asian cities contrasts with the poor performance in Southeast Asian urban centers, despite the latter region's disproportionate vulnerability to heat impacts. This disparity may reflect differences in the density and quality of observational networks used for model validation, the complexity of regional climate systems influenced by monsoon dynamics and maritime effects, or fundamental limitations in representing tropical urban climates. Recent research confirms that bias-corrected multi-model ensembles project substantial warming and wetting across mainland Southeast Asian countries, with temperature increases ranging from 1.88-4.22°C by the end of the century depending on scenario and location, but the reliability of these projections remains questionable given the systematic biases documented in this analysis.

## Conclusion

This evaluation of CMIP6 model performance across Asian cities, with comparison to GHCND observations and ERA5 reanalysis data, reveals challenges in applying global climate models to urban-scale assessments, particularly in tropical and subtropical regions. The strong latitudinal gradient in performance, with models performing well in temperate and arid regions but poorly in tropical environments, indicates a need for the continuing development of models to better represent the physical dynamics of these climate zones.

Future research priorities should focus on several key areas. First, the development of urban-aware parameterizations in global climate models could help address the systematic biases observed across different Local Climate Zones and urban morphologies. Second, expanded observational networks in Southeast Asian cities would enable more robust validation of model performance and bias correction procedures in the regions most vulnerable to heat impacts. Third, advanced statistical and dynamical downscaling approaches, potentially leveraging machine learning techniques, could bridge the scale gap between coarse global models and fine-scale urban climate processes. Fourth, ensemble approaches that account for model structural uncertainty and weight models based on performance in specific climate and urban contexts could provide more reliable projections for adaptation planning.

The implications of these findings extend beyond technical model evaluation to fundamental questions about climate justice and adaptation capacity. Poor model performance in regions experiencing the most rapid urbanization and highest heat vulnerability creates a knowledge gap precisely where reliable climate information is most urgently needed. As urban populations continue to grow and climate change intensifies heat extremes, the ability to accurately project future temperature conditions in Asian cities will become increasingly critical for designing effective adaptation strategies, protecting vulnerable populations, and ensuring sustainable urban development. This evaluation demonstrates both the progress achieved through CMIP6 and the substantial work remaining to provide urban planners, public health officials, and policymakers with the reliable, locally relevant climate information they require to build resilient cities in the era of anthropogenic climate change.

Several limitations should be acknowledged in interpreting these results. First, our analysis focuses primarily on temperature variables, and model performance for precipitation and other variables may show different patterns. Second, the station selection criteria may introduce sampling biases toward urban and densely populated areas, potentially limiting the representativeness of our findings for rural or remote regions. Third, the focus on daily timescales may not capture model performance at sub-daily or longer timescales that are relevant for different applications. Future work should extend this analysis to include precipitation variables, examine model performance at multiple timescales, and investigate the relationship between model performance and specific physical parameterizations.

## Appendix

**Extended Data Table 1 |** Distribution of study cities by Local Climate Zone (LCZ).

| lcz_zone | lcz_zone_count |
|---|---|
| Compact_mid-rise | 116 |
| Compact_low-rise | 98 |
| Large_low-rise | 72 |
| Open_low-rise | 37 |
| Open_high-rise | 30 |
| Open_mid-rise | 24 |
| Compact_high-rise | 16 |
| Heavy_industry | 10 |
| Water | 4 |
| Sparsely_built | 4 |
| Dense_trees | 2 |
| Low_plants | 2 |
| Bare_soil_sand | 1 |
| Lightweight_low-rise | 1 |

**Extended Data Table 2 |** Distribution of study cities by Köppen–Geiger climate zone.

| koppen_zone | koppen_zone_count |
|---|---|
| Temperate_no_dry_hot | 93 |
| Temperate_dry_winter_hot | 76 |
| Tropical_savannah | 45 |
| Cold_dry_winter_hot | 42 |
| Arid_steppe_cold | 33 |
| Arid_steppe_hot | 26 |
| Arid_desert_hot | 23 |
| Tropical_monsoon | 23 |
| Tropical_rainforest | 22 |
| Temperate_dry_summer_hot | 19 |
| Arid_desert_cold | 6 |
| Temperate_dry_winter_warm | 4 |
| Cold_no_dry_warm | 2 |
| Cold_no_dry_hot | 1 |
| Cold_dry_winter_cold | 1 |
| Temperate_no_dry_warm | 1 |

**Extended Data Table 3 |** Distribution of study cities by terrestrial biome.

| BIOME_NAME | BIOME_NAME_count |
|---|---|
| Temperate Broadleaf & Mixed Forests | 148 |
| Tropical & Subtropical Moist Broadleaf Forests | 128 |
| Deserts & Xeric Shrublands | 43 |
| Tropical & Subtropical Dry Broadleaf Forests | 28 |
| Mediterranean Forests, Woodlands & Scrub | 19 |
| Temperate Grasslands, Savannas & Shrublands | 19 |
| Mangroves | 4 |
| Temperate Conifer Forests | 4 |
| Tropical & Subtropical Grasslands, Savannas & Shrublands | 2 |
| Montane Grasslands & Shrublands | 2 |
| Tropical & Subtropical Coniferous Forests | 1 |

**Extended Data Table 4 |** Distribution of study cities by biogeographic realm.

| REALM | REALM_count |
|---|---|
| Palearctic | 216 |
| Indomalayan | 177 |
| Afrotropic | 4 |
| Australasia | 1 |

## References


Abulibdeh, A. Analysis of urban heat island characteristics and mitigation strategies for eight arid and semi-arid gulf region cities. *Environ Earth Sci* **80**, 259 (2021). https://doi.org/10.1007/s12665-021-09540-7

Alahmad, B., Lung, SC.C., Makar, A. *et al.* Heat stress and productivity losses in urban construction workforces. *Nat Cities* **2**, 703–707 (2025). https://doi.org/10.1038/s44284-025-00283-1

Almazroui, M., Saeed, F., Saeed, S., Nazrul Islam, M., Ismail, M., Klutse, N. A., & Siddiqui, M. H. (2020). Projected change in temperature and precipitation over Africa from CMIP6. *Earth Systems and Environment*, 4(3), 455-475. doi:10.1007/s41748-020-00161-x

Almeida, C. R. d., Teodoro, A. C., & Gonçalves, A. (2021). Study of the Urban Heat Island (UHI) Using Remote Sensing Data/Techniques: A Systematic Review. *Environments*, *8*(10), 105. https://doi.org/10.3390/environments8100105

Azad, N., Ahmadi, A. Assessment of CMIP6 models and multi-model averaging for temperature and precipitation over Iran. Sci Rep 14, 24165 (2024). https://doi.org/10.1038/s41598-024-74789-4

Bhanage, V., Lee, H. S., Kubota, T., Pradana, R. P., Fajary, F. R., Arya Putra, I. D. G., & Nimiya, H. (2023). City-Wise Assessment of Suitable CMIP6 GCM in Simulating Different Urban Meteorological Variables over Major Cities in Indonesia. Climate, 11(5), 100. https://doi.org/10.3390/cli11050100

Bhanage V. , Lee Han Soo , Cabrera Jonathan Salar , Kubota Tetsu , Pradana Radyan Putra , Fajary Faiz Rohman , Nimiya Hideyo ; Identification of optimal CMIP6 GCMs for future typical meteorological year in major cities of Indonesia using multi-criteria decision analysis ; Frontiers in Environmental Science ; Volume 12 – 2024 ; 2024 ; https://www.frontiersin.org/journals/environmental-science/articles/10.3389/fenvs.2024.1341807 ; DOI=10.3389/fenvs.2024.1341807

Cheval, S., Vlad-Alexandru Amihăesei, Zenaida Chitu, Alexandru Dumitrescu, Vladut Falcescu, Adrian Irașoc, Dana Magdalena Micu, Eugen Mihulet, Irina Ontel, Monica-Gabriela Paraschiv, Nicu Constantin Tudose, A systematic review of urban heat island and heat waves research (1991–2022), Climate Risk Management, Volume 44, 2024, 100603, ISSN 2212-0963, https://doi.org/10.1016/j.crm.2024.100603.

Choi, Y., Lee, S., & Moon, H. (2018). Urban Physical Environments and the Duration of High Air Temperature: Focusing on Solar Radiation Trapping Effects. *Sustainability*, *10*(12), 4837. https://doi.org/10.3390/su10124837

Climate Impact Tracker. (2025). The 2025 Heatwave in Southeast Asia: A Window Into the Future. Retrieved from https://www.climateimpactstracker.com/2025-heatwave-in-southeast-asia/

Craigmile, P. F., & Guttorp, P. (2023). Comparing CMIP6 climate model simulations of annual global mean temperatures to a new combined data product. *Earth and Space Science*, 10, e2022EA002468. https://doi.org/10.1029/2022EA002468

Cui, T., Li, C., & Tian, F. (2021). Evaluation of temperature and precipitation simulations in CMIP6 models over the Tibetan Plateau. *Earth and Space Science*, 8, e2020EA001620. https://doi.org/10.1029/2020EA001620

Dai, A. (2006). Precipitation characteristics in eighteen coupled climate models. *Journal of Climate*, 19(18), 4605-4630. https://doi.org/10.1175/JCLI3884.1

Delgado-Torres, C., and Coauthors, 2022: Multi-Model Forecast Quality Assessment of CMIP6 Decadal Predictions. *J. Climate*, **35**, 4363–4382, https://doi.org/10.1175/JCLI-D-21-0811.1.

Desmet, Q., & Ngo-Duc, T. (2022). A novel method for ranking CMIP6 global climate models over the southeast Asian region. *International Journal of Climatology*, 42(1), 97–117. https://doi.org/10.1002/joc.7234

Eunice Lo, Y.T., Vosper, E., Higgins, J.P.T, Howard, G. (2024). Heat impacts on human health in the Western Pacific Region: An umbrella review. *The Lancet Regional Health - Western Pacific*, 42, 100952. https://www.thelancet.com/journals/lanwpc/article/PIIS2666-6065(23)00270-5/fulltext

Eyring, V., Bony, S., Meehl, G. A., Senior, C. A., Stevens, B., Stouffer, R. J., & Taylor, K. E. (2016). Overview of the Coupled Model Intercomparison Project Phase 6 (CMIP6) experimental design and organization. *Geoscientific Model Development*, 9(5), 1937-1958. https://gmd.copernicus.org/articles/9/1937/2016/

Fan, X., Duan, Q., Shen, C., Wu, Y., & Xing, C. (2020). Global surface air temperatures in CMIP6: Historical performance and future changes. *Environmental Research Letters*, 15(10), 104056. DOI 10.1088/1748-9326/abb051

Flato, G., Marotzke, J., Abiodun, B., Braconnot, P., Chou, S. C., Collins, W., ... & Rummukainen, M. (2013). Evaluation of climate models. In *Climate change 2013: the physical science basis. Contribution of working group I to the fifth assessment report of the intergovernmental panel on climate change* (pp. 741-866). Cambridge University Press. https://www.ipcc.ch/site/assets/uploads/2018/02/WG1AR5_Chapter09_FINAL.pdf

Flouris AD, Dinas PC, Ioannou LG, Nybo L, Havenith G, Kenny GP, Kjellstrom T. Workers' health and productivity under occupational heat strain: a systematic review and meta-analysis. Lancet Planet Health. 2018 Dec;2(12):e521-e531. doi: 10.1016/S2542-5196(18)30237-7. PMID: 30526938.

Forster, P. M., Smith, C., Walsh, T., Lamb, W. F., Lamboll, R., Cassou, C., Hauser, M., Hausfather, Z., Lee, J.-Y., Palmer, M. D., von Schuckmann, K., Slangen, A. B. A., Szopa, S., Trewin, B., Yun, J., Gillett, N. P., Jenkins, S., Matthews, H. D., Raghavan, K., Ribes, A., Rogelj, J., Rosen, D., Zhang, X., Allen, M., Aleluia Reis, L., Andrew, R. M., Betts, R. A., Borger, A., Broersma, J. A., Burgess, S. N., Cheng, L., Friedlingstein, P., Domingues, C. M., Gambarini, M., Gasser, T., Gütschow, J., Ishii, M., Kadow, C., Kennedy, J., Killick, R. E., Krummel, P. B., Liné, A., Monselesan, D. P., Morice, C., Mühle, J., Naik, V., Peters, G. P., Pirani, A., Pongratz, J., Minx, J. C., Rigby, M., Rohde, R., Savita, A., Seneviratne, S. I., Thorne, P., Wells, C., Western, L. M., van der Werf, G. R., Wijffels, S. E., Masson-Delmotte, V., and Zhai, P.: Indicators of Global Climate Change 2024: annual update of key indicators of the state of the climate system and human influence, Earth Syst. Sci. Data, 17, 2641–2680, https://doi.org/10.5194/essd-17-2641-2025.

Gao, S., Chen, Y., Chen, D. *et al.* Urbanization-induced warming amplifies population exposure to compound heatwaves but narrows exposure inequality between global North and South cities. *npj Clim Atmos Sci* **7**, 154 (2024). https://doi.org/10.1038/s41612-024-00708-z

Gebrechorkos, S., Leyland, J., Slater, L. *et al.* A high-resolution daily global dataset of statistically downscaled CMIP6 models for climate impact analyses. *Sci Data* **10**, 611 (2023). https://doi.org/10.1038/s41597-023-02528-x

Goyal, M.K., Gupta, A.K., Das, J. et al. Heatwave magnitude impact over Indian cities: CMIP 6 projections. Theor Appl Climatol 154, 959–971 (2023). https://doi.org/10.1007/s00704-023-04599-7

Gusain, A., Ghosh, S., & Karmakar, S. (2020). Added value of CMIP6 over CMIP5 models in simulating Indian summer monsoon rainfall. *Atmospheric Research*, 232, 104680. https://doi.org/10.1016/j.atmosres.2019.104680

Hamed, M. M., Mohamed Salem Nashwan, Shamsuddin Shahid, Tarmizi bin Ismail, Xiaojun Wang, Ashraf Dewan, Md Asaduzzaman, Inconsistency in historical simulations and future projections of temperature and rainfall: A comparison of CMIP5 and CMIP6 models over Southeast Asia, Atmospheric Research, Volume 265, 2022, 105927, ISSN 0169-8095, https://doi.org/10.1016/j.atmosres.2021.105927.

Hassan, T., Zhang, J., Prodhan, F. A., Pangali Sharma, T. P., & Bashir, B. (2021). Surface Urban Heat Islands Dynamics in Response to LULC and Vegetation across South Asia (2000–2019). *Remote Sensing*, *13*(16), 3177. https://doi.org/10.3390/rs13163177

Hawkins, E., & Sutton, R. (2009). The potential to narrow uncertainty in regional climate predictions. *Bulletin of the American Meteorological Society*, 90(8), 1095-1108. https://journals.ametsoc.org/view/journals/bams/90/8/2009bams2607_1.xml

Hersbach, H., Bell, B., Berrisford, P., Hirahara, S., Horányi, A., Muñoz-Sabater, J., ... & Thépaut, J. N. (2020). The ERA5 global reanalysis. *Quarterly Journal of the Royal Meteorological Society*, 146(730), 1999-2049. https://rmets.onlinelibrary.wiley.com/doi/10.1002/qj.3803

Hijioka, Y., Lin, E., Pereira, J.J., Corlett, R.T., Cui, X., Insarov, G.E., Lasco, R.D., Lindgren, E. and Surjan, A. (2014) Asia. In: Barros, V.R., Field, C.B., Dokken, D.J., Mastrandrea, M.D., Mach, K.J., Bilir, T.E., Chatterjee, M., Ebi, K.L., Estrada, Y.O., Genova, R.C., Girma, B., Kissel, E.S., Levy, A.N., MacCracken, S., Mastrandrea, P.R. and White, L.L., Eds., Climate Change 2014: Impacts, Adaptation, and Vulnerability. Part B: Regional Aspects. Contribution of Working Group II to the Fifth Assessment Report of the Intergovernmental Panel on Climate Change, Cambridge University Press, Cambridge, 1327-1370. https://www.ipcc.ch/site/assets/uploads/2018/02/WGIIAR5-Chap24_FINAL.pdf

Hirsch, A. L., Ridder, N. N., Perkins-Kirkpatrick, S. E., & Ukkola, A. (2021). CMIP6 multimodel evaluation of present-day heatwave attributes. *Geophysical Research Letters*, 48, e2021GL095161. https://doi.org/10.1029/2021GL095161

Hoegh-Guldberg, O., Jacob, D., Taylor, M., Bindi, M., Brown, S., Camilloni, I., ... & Zhou, G. (2018). Impacts of 1.5°C global warming on natural and human systems. In *Global warming of 1.5°C. An IPCC Special Report* (pp. 175-311). Cambridge University Press. https://www.ipcc.ch/site/assets/uploads/sites/2/2019/02/SR15_Chapter3_Low_Res.pdf

IPCC. (2021). Climate change widespread, rapid, and intensifying. Press release. Retrieved from https://www.ipcc.ch/2021/08/09/ar6-wg1-20210809-pr/

IPCC. 2021b: Summary for Policymakers. In: *Climate Change 2021: The Physical Science Basis. Contribution of Working Group I to the Sixth Assessment Report of the Intergovernmental Panel on Climate Change* [Masson-Delmotte, V., P. Zhai, A. Pirani, S.L. Connors, C. Péan, S. Berger, N. Caud, Y. Chen, L. Goldfarb, M.I. Gomis, M. Huang, K. Leitzell, E. Lonnoy, J.B.R. Matthews, T.K. Maycock, T. Waterfield, O. Yelekçi, R. Yu, and B. Zhou (eds.)]. In Press. https://www.ipcc.ch/report/ar6/wg1/downloads/report/IPCC_AR6_WGI_SummaryVolume.pdf

IPCC. (2024). IPCC statements and press releases. Retrieved from https://www.ipcc.ch/2024/

International Energy Agency. (2025). Global Energy Review 2025: CO2 Emissions. Paris: IEA. Available at: https://www.iea.org/reports/global-energy-review-2025/co2-emissions

International Monetary Fund. (2024). Regional Economic Outlook for Asia and Pacific, October 2024: Resilient Growth but Higher Risks. Washington, DC: IMF. Available at: https://www.imf.org/en/Publications/REO/APAC/Issues/2024/10/31/regional-economic-outlook-for-asia-and-pacific-october-2024

Islam, S., Karipot, A., Bhawar, R. *et al.* Urban heat island effect in India: a review of current status, impact and mitigation strategies. *Discov Cities* **1**, 34 (2024). https://doi.org/10.1007/s44327-024-00033-3

Jose, D.M., Dwarakish, G.S. Bias Correction and Trend Analysis of Temperature Data by a High-Resolution CMIP6 Model over a Tropical River Basin. Asia-Pacific J Atmos Sci 58, 97–115 (2022). https://doi.org/10.1007/s13143-021-00240-7

Kim, Y., Seung-Ki Min, Xuebin Zhang, Jana Sillmann, Marit Sandstad, Evaluation of the CMIP6 multi-model ensemble for climate extreme indices, Weather and Climate Extremes, Volume 29, 2020, 100269, ISSN 2212-0947, https://doi.org/10.1016/j.wace.2020.100269.

Kong Q, Huber M. A global high-resolution and bias-corrected dataset of CMIP6 projected heat stress metrics. Sci Data. 2025 Feb 12;12(1):246. doi: 10.1038/s41597-025-04527-6. PMID: 39939321; PMCID: PMC11821900.

Kooperman, G. J., Pritchard, M. S., Burt, M. A., Branson, M. D., & Randall, D. A. (2018). Robust effects of cloud superparameterization on simulated daily rainfall intensity statistics across multiple versions of the Community Earth System Model. *Journal of Advances in Modeling Earth Systems*, 10(12), 3030-3049. https://doi.org/10.1002/2015MS000574

Kotharkar, R., Aparna Ramesh, Anurag Bagade, Urban Heat Island studies in South Asia: A critical review, Urban Climate, Volume 24, 2018, Pages 1011-1026, ISSN 2212-0955, https://doi.org/10.1016/j.uclim.2017.12.006.

Kumar, R., Mishra, V., Buzan, J., Kumar, R., Shindell, D., & Huber, M. (2017). Dominant control of agriculture and irrigation on urban heat island in India. *Scientific Reports*, 7:14054. doi: 10.1038/s41598-017-14213-2

Kumar, P., Barat, A., Sarthi, P.P. *et al.* Evaluating future urban temperature over smart cities of the Gangetic plains using statistically downscaled CMIP6 projections. *Theor Appl Climatol* **155**, 4585–4600 (2024). https://doi.org/10.1007/s00704-024-04896-9

Lafferty, D.C., Sriver, R.L. Downscaling and bias-correction contribute considerable uncertainty to local climate projections in CMIP6. *npj Clim Atmos Sci* **6**, 158 (2023). https://doi.org/10.1038/s41612-023-00486-0

Lalande, M., Ménégoz, M., Krinner, G., Naegeli, K., and Wunderle, S.: Climate change in the High Mountain Asia in CMIP6, Earth Syst. Dynam., 12, 1061–1098, https://doi.org/10.5194/esd-12-1061-2021.

Lawrimore, J. H., Menne, M. J., Gleason, B. E., Williams, C. N., Wuertz, D. B., Vose, R. S., & Rennie, J. (2011). An overview of the Global Historical Climatology Network monthly mean temperature data set, version 3. *Journal of Geophysical Research: Atmospheres*, 116(D19). https://agupubs.onlinelibrary.wiley.com/doi/abs/10.1029/2011jd016187

Li, X., Li, Z. Evaluation of bias correction techniques for generating high-resolution daily temperature projections from CMIP6 models. Clim Dyn 61, 3893–3910 (2023). https://doi.org/10.1007/s00382-023-06778-8

Liu, F., Xu, C., Long, Y., Yin, G., & Wang, H. (2022). Assessment of CMIP6 Model Performance for Air Temperature in the Arid Region of Northwest China and Subregions. *Atmosphere*, *13*(3), 454. https://doi.org/10.3390/atmos13030454

Lowe D, Ebi KL, Forsberg B. Heatwave early warning systems and adaptation advice to reduce human health consequences of heatwaves. Int J Environ Res Public Health. 2011 Dec;8(12):4623-48. doi: 10.3390/ijerph8124623. Epub 2011 Dec 12. PMID: 22408593; PMCID: PMC3290979.

Lowe, R., Ballester, J., Creswick, J., Robine, J. M., Herrmann, F. R., & Rodó, X. (2018). Evaluating the performance of a climate-driven mortality model during heat waves and cold spells in Europe. *International Journal of Environmental Research and Public Health*, 15(9), 1279. https://pubmed.ncbi.nlm.nih.gov/25625407/

LUO, N., GUO, Y., GAO, Z., CHEN, K., & CHOU, J. (2020). Assessment of CMIP6 and CMIP5 model performance for extreme temperature in China. Atmospheric and Oceanic Science Letters, 13(6), 589–597. https://doi.org/10.1080/16742834.2020.1808430

Jung, Y. (2024). Urban heat islands and the transformation of Singapore. *Urban Studies*, *61*(15), 2908-2927. https://doi.org/10.1177/00420980231217391

Maharjan, M., Aryal, A., Man Shakya, B., Talchabhadel, R., Thapa, B. R., & Kumar, S. (2021). Evaluation of Urban Heat Island (UHI) Using Satellite Images in Densely Populated Cities of South Asia. *Earth*, *2*(1), 86-110. https://doi.org/10.3390/earth2010006

Manoli, G., Fatichi, S., Schläpfer, M. *et al.* Magnitude of urban heat islands largely explained by climate and population. *Nature* **573**, 55–60 (2019). https://doi.org/10.1038/s41586-019-1512-9

Maraun, D., & Widmann, M. (2018). *Statistical downscaling and bias correction for climate research*. Cambridge University Press. https://doi.org/10.1017/9781107588783

Mauritsen, T., & Stevens, B. (2015). Missing iris effect as a possible cause of muted hydrological change and high climate sensitivity in models. *Nature Geoscience*, 8(5), 346-351. doi:10.1038/ngeo2414

McKinsey Global Institute. (2023). Asia on the cusp of a new era. https://www.mckinsey.com/mgi/our-research/asia-on-the-cusp-of-a-new-era#/

Meade, R.D., Sean R. Notley, Ashley P. Akerman, James J. McCormick, Kelli E. King, Ronald J. Sigal and Glen P. Kenny; Efficacy of Cooling Centers for Mitigating Physiological Strain in Older Adults during Daylong Heat Exposure: A Laboratory-Based Heat Wave Simulation; Environmental Health Perspectives; 131, 6, 067003, 2023, https://doi.org/10.1289/EHP11651

Menne, M. J., Durre, I., Vose, R. S., Gleason, B. E., & Houston, T. G. (2012). An overview of the Global Historical Climatology Network-Daily database. *Journal of Atmospheric and Oceanic Technology*, 29(7), 897-910. https://journals.ametsoc.org/view/journals/atot/29/7/jtech-d-11-00103_1.xml

Mohajerani, A., Bakaric, J. and Jeffrey-Bailey, T. (2017) The Urban Heat Island Effect, Its Causes, and Mitigation, with Reference to the Thermal Properties of Asphalt Concrete. Journal of Environmental Management, 197, 522-538. https://doi.org/10.1016/j.jenvman.2017.03.095

Mousavikhaledi, O., Firoozzare, A., Boccia, F. et al. Multi-model ensemble CMIP6 for prediction of climate changes: evidence from Asia. Environ Dev Sustain (2025). https://doi.org/10.1007/s10668-025-06371-5

Mueller, B., & Seneviratne, S. I. (2012). Hot days induced by precipitation deficits at the global scale. *Proceedings of the National Academy of Sciences*, 109(31), 12398-12403. https://doi.org/10.1073/pnas.1204330109

Nguyen, C.T., Chidthaisong, A., Kaewthongrach, R., Marome, W. (2023). Urban Thermal Environment Under Urban Expansion and Climate Change: A Regional Perspective from Southeast Asian Big Cities. In: Cheshmehzangi, A., He, BJ., Sharifi, A., Matzarakis, A. (eds) Climate Change and Cooling Cities. Urban Sustainability. Springer, Singapore. https://doi.org/10.1007/978-981-99-3675-5_9

O'Neill, B. C., Tebaldi, C., van Vuuren, D. P., Eyring, V., Friedlingstein, P., Hurtt, G., ... & Sanderson, B. M. (2016). The scenario model intercomparison project (ScenarioMIP) for CMIP6. *Geoscientific Model Development*, 9(9), 3461-3482. https://doi.org/10.5194/gmd-9-3461-2016

Pan, H., Hai Lin, Yi Xu, Yi Yang, Future projections of temperature extremes over East Asia based on a deep learning downscaled CMIP6 high-resolution (0.1°) dataset, Atmospheric Research, Volume 305, 2024, 107448, ISSN 0169-8095, https://doi.org/10.1016/j.atmosres.2024.107448.

Pavanello, F., De Cian, E., Davide, M. *et al.* Air-conditioning and the adaptation cooling deficit in emerging economies. *Nat Commun* **12**, 6460 (2021). https://doi.org/10.1038/s41467-021-26592-2

Pepin, N., Bradley, R. S., Diaz, H. F., Baraer, M., Caceres, E. B., Forsythe, N., ... & Yang, D. Q. (2015). Elevation-dependent warming in mountain regions of the world. *Nature Climate Change*, 5(5), 424-430. https://doi.org/10.1038/nclimate2563

Perkins-Kirkpatrick, S. E., & Lewis, S. C. (2020). Increasing trends in regional heatwaves. *Nature Communications*, 11(1), 3357. https://www.nature.com/articles/s41467-020-16970-7

Piracha, A., & Chaudhary, M. T. (2022). Urban Air Pollution, Urban Heat Island and Human Health: A Review of the Literature. *Sustainability*, *14*(15), 9234. https://doi.org/10.3390/su14159234

Papalexiou, S. M., Rajulapati, C. R., Clark, M. P., & Lehner, F. (2020). Robustness of CMIP6 historical global mean temperature simulations: Trends, long-term persistence, autocorrelation, and distributional shape. *Earth's Future*, 8, e2020EF001667. https://doi.org/10.1029/2020EF001667

Rampal, N., and Coauthors, 2024: Enhancing Regional Climate Downscaling through Advances in Machine Learning. *Artif. Intell. Earth Syst.*, **3**, 230066, https://doi.org/10.1175/AIES-D-23-0066.1.

Ren, G., Y. Zhou, Z. Chu, J. Zhou, A. Zhang, J. Guo, and X. Liu, 2008: Urbanization Effects on Observed Surface Air Temperature Trends in North China. *J. Climate*, **21**, 1333–1348, https://doi.org/10.1175/2007JCLI1348.1.

Reyes-García, V., García-del-Amo, D., Álvarez-Fernández, S. et al. Indigenous Peoples and local communities report ongoing and widespread climate change impacts on local social-ecological systems. Commun Earth Environ 5, 29 (2024). https://doi.org/10.1038/s43247-023-01164-y

Roshan G, Sarli R, Grab SW. The case of Tehran's urban heat island, Iran: Impacts of urban 'lockdown' associated with the COVID-19 pandemic. Sustain Cities Soc. 2021 Dec;75:103263. doi: 10.1016/j.scs.2021.103263. Epub 2021 Aug 14. PMID: 36568531; PMCID: PMC9760287.

Rostron, J. W., Sexton, D. M., McSweeney, C. F., Yamazaki, K., Andrews, T., Ringer, M. A., ... & Tsushima, Y. (2020). The impact of performance filtering on climate feedbacks in a perturbed parameter ensemble. *Climate Dynamics*, 55(3), 521-551. https://doi.org/10.1007/s00382-020-05281-8

Rummukainen, M. (2010), State-of-the-art with regional climate models. WIREs Clim Change, 1: 82-96. https://doi.org/10.1002/wcc.8

Rupa Basu, Jonathan M. Samet, Relation between Elevated Ambient Temperature and Mortality: A Review of the Epidemiologic Evidence, *Epidemiologic Reviews*, Volume 24, Issue 2, December 2002, Pages 190–202, https://doi.org/10.1093/epirev/mxf007

Saffari, M., Alvaro de Gracia, Svetlana Ushak, Luisa F. Cabeza, Passive cooling of buildings with phase change materials using whole-building energy simulation tools: A review; Renewable and Sustainable Energy Reviews, Volume 80, 2017, Pages 1239-1255, ISSN 1364-0321, https://doi.org/10.1016/j.rser.2017.05.139.

Sanderson, B. M., Knutti, R., & Caldwell, P. (2015). A representative democracy to reduce interdependency in a multimodel ensemble. *Journal of Climate*, 28(13), 5171-5194. https://doi.org/10.1175/JCLI-D-14-00362.1

Scafetta, N. CMIP6 GCM ensemble members versus global surface temperatures. *Clim Dyn* **60**, 3091–3120 (2023). https://doi.org/10.1007/s00382-022-06493-w

Seneviratne, S.I., X. Zhang, M. Adnan, W. Badi, C. Dereczynski, A. Di Luca, S. Ghosh, I. Iskandar, J. Kossin, S. Lewis, F. Otto, I. Pinto, M. Satoh, S.M. Vicente-Serrano, M. Wehner, and B. Zhou,2021: Weather and Climate Extreme Events in a Changing Climate. In Climate Change 2021: The Physical Science Basis. Contribution of Working Group I to the Sixth Assessment Report of the Intergovernmental Panel on Climate Change [Masson-Delmotte, V., P. Zhai, A. Pirani, S.L. Connors, C. Péan, S. Berger, N. Caud, Y. Chen, L. Goldfarb, M.I. Gomis, M. Huang, K. Leitzell, E. Lonnoy, J.B.R. Matthews, T.K. Maycock, T. Waterfield, O. Yelekçi, R. Yu, and B. Zhou (eds.)]. Cambridge University Press, Cambridge, United Kingdom and New York, NY, USA, pp. 1513–1766, doi:10.1017/9781009157896.013.

Shaw, R., Y. Luo, T.S. Cheong, S. Abdul Halim, S. Chaturvedi, M. Hashizume, G.E. Insarov, Y. Ishikawa, M. Jafari, A. Kitoh, J. Pulhin, C. Singh, K. Vasant, and Z. Zhang, 2022: Asia. In: Climate Change 2022: Impacts, Adaptation and Vulnerability. Contribution of Working Group II to the Sixth Assessment Report of the Intergovernmental Panel on Climate Change [H.-O. Pörtner, D.C. Roberts, M. Tignor, E.S. Poloczanska, K. Mintenbeck, A. Alegría, M. Craig, S. Langsdorf, S. Löschke, V. Möller, A. Okem, B. Rama (eds.)]. Cambridge University Press, Cambridge, UK and New York, NY, USA, pp. 1457–1579, doi:10.1017/9781009325844.012.

Sherwood, S. C., Webb, M. J., Annan, J. D., Armour, K. C., Forster, P. M., Hargreaves, J. C., ... & Zelinka, M. D. (2020). An assessment of Earth's climate sensitivity using multiple lines of evidence. *Reviews of Geophysics*, 58(4), e2019RG000678. https://doi.org/10.1029/2019RG000678

Singh, S., R.K. Mall, Praveen K. Singh, R. Bhatla, Pawan K. Chaubey, How virtuous are the bias corrected CMIP6 models in the simulation of heatwave over different meteorological subdivisions of India?, Urban Climate, Volume 55, 2024, 101936, ISSN 2212-0955, https://doi.org/10.1016/j.uclim.2024.101936.

Sofer, M., Potchter, O. The urban heat island of a city in an arid zone: the case of Eilat, Israel. *Theor. Appl. Climatol.* **85**, 81–88 (2006). https://doi.org/10.1007/s00704-005-0181-9

Supharatid, S., J. Nafung, T. Aribarg; Projected changes in temperature and precipitation over mainland Southeast Asia by CMIP6 models. Journal of Water and Climate Change 1 January 2022; 13 (1): 337–356. doi: https://doi.org/10.2166/wcc.2021.015

Takane, Y., Kikegawa, Y., Hara, M. *et al.* Urban warming and future air-conditioning use in an Asian megacity: importance of positive feedback. *npj Clim Atmos Sci* **2**, 39 (2019). https://doi.org/10.1038/s41612-019-0096-2

Tapiador, F. J., Turk, F. J., Petersen, W., Hou, A. Y., García-Ortega, E., Machado, L. A., ... & de Castro, M. (2012). Global precipitation measurement: Methods, datasets and applications. *Atmospheric Research*, 104, 70-97. doi:10.1016/j.atmosres.2011.10.021

Teutschbein, C., & Seibert, J. (2012). Bias correction of regional climate model simulations for hydrological climate-change impact studies: Review and evaluation of different methods. *Journal of Hydrology*, 456, 12-29. https://doi.org/10.1016/j.jhydrol.2012.05.052

Try, S., & Qin, X. (2024). Evaluation of Future Changes in Climate Extremes over Southeast Asia Using Downscaled CMIP6 GCM Projections. Water, 16(15), 2207. https://doi.org/10.3390/w16152207

Turek-Hankins, L. L., Coughlan de Perez, E., Scarpa, G., Ruiz-Diaz, R., Naik, N., Wannewitz, M., ... & Singh, C. (2021). Climate change adaptation to extreme heat: A global systematic review of implemented action. *Oxford Open Climate Change*, 1(1), kgab005. https://eprints.gla.ac.uk/257803/1/257803.pdf

Tzyrkalli, A., Economou, T., Lazoglou, G., Constantinidou, K., Hadjinicolaou, P., & Lelieveld, J. (2024). Urban Heat Island Trends in the Middle East and North Africa: A statistical approach. *International Journal of Climatology*, 44(11), 3998–4008. https://doi.org/10.1002/joc.8563

Ulpiani G. On the linkage between urban heat island and urban pollution island: Three-decade literature review towards a conceptual framework. Sci Total Environ. 2021 Jan 10;751:141727. doi: 10.1016/j.scitotenv.2020.141727. Epub 2020 Aug 18. PMID: 32890803; PMCID: PMC7434321.

United Nations. (2024). *The Sustainable Development Goals Report 2024*. United Nations Publications. https://unstats.un.org/sdgs/report/2024/

United Nations. (2024). 1.5°C: What it means and why it matters. UN Climate Change. Retrieved from https://www.un.org/en/climatechange/science/climate-issues/degrees-matter

United Nations. (2024b). World Population Prospects 2024: Summary of Results. New York: United Nations. United Nations, Department of Economic and Social Affairs, Population Division. Available at: https://population.un.org/wpp/

United Nations Environment Programme. (n.d.). In South Asia, record heat threatens future of farming. Retrieved from https://www.unep.org/news-and-stories/story/south-asia-record-heat-threatens-future-farming

United States Institute of Peace. (2024). How heat waves are destabilizing Asia. Retrieved from https://www.usip.org/publications/2023/06/how-heat-waves-are-destabilizing-asia

U.S. Environmental Protection Agency. (2025). Using cool pavements to reduce heat islands. Retrieved from https://www.epa.gov/heatislands/using-cool-pavements-reduce-heat-islands

Vial, J., Dufresne, J. L., & Bony, S. (2013). On the interpretation of inter-model spread in CMIP5 climate sensitivity estimates. *Climate Dynamics*, 41(11-12), 3339-3362. doi:10.1007/s00382-013-1725-9

Vu, A., Felicity Kersting, Sherman Tai, Jonathan Rigg, and Ekaterina Tarnovskaya. 2025. Impacts of Climate Change on the Health of Outdoor Workers in Urban Asia. National Centre for Social Research. https://natcen.ac.uk/publications/impacts-climate-change-health-outdoor-workers-urban-asia

Watts, N., Amann, M., Arnell, N., Ayeb-Karlsson, S., Beagley, J., Belesova, K., ... & Costello, A. (2021). The 2020 report of The Lancet Countdown on health and climate change: responding to converging crises. *The Lancet*, 397(10269), 129-170. https://pubmed.ncbi.nlm.nih.gov/33278353/

Wang, K., Aktas, Y.D., Stocker, J. *et al.* Urban heat island modelling of a tropical city: case of Kuala Lumpur. *Geosci. Lett.* **6**, 4 (2019). https://doi.org/10.1186/s40562-019-0134-2

Williams, K. D., Copsey, D., Blockley, E. W., Bodas-Salcedo, A., Calvert, D., Comer, R., ... & Woodhouse, M. T. (2018). The Met Office Global Coupled Model 3.0 and 3.1 (GC3.0 and GC3.1) configurations. *Journal of Advances in Modeling Earth Systems*, 10(2), 357-380. https://doi.org/10.1002/2017MS001115

World Bank. (2023). Unlivable: What the Urban Heat Island Effect Means for East Asia's Cities. https://www.worldbank.org/en/region/eap/publication/unlivable-what-the-urban-heat-island-effect-means-for-east-asia-s-cities

World Health Organization. (2024). Heat and health. Retrieved from https://www.who.int/news-room/fact-sheets/detail/climate-change-heat-and-health

World Meteorological Organization. (2019). WMO verifies 3rd and 4th hottest temperature recorded on Earth. Retrieved from https://web.archive.org/web/20231218172054/https://public-old.wmo.int/en/media/press-release/wmo-verifies-3rd-and-4th-hottest-temperature-recorded-earth

World Meteorological Organization. (2025). *State of the Global Climate 2024*. WMO-No. 1368.

World Meteorological Organization. (2025). Global climate predictions show temperatures expected to remain at or near record levels in coming 5 years. Retrieved from https://wmo.int/news/media-centre/global-climate-predictions-show-temperatures-expected-remain-or-near-record-levels-coming-5-years

World Meteorological Organization. (2025b). Rising temperatures and extreme weather hit Asia hard. Retrieved from https://wmo.int/news/media-centre/rising-temperatures-and-extreme-weather-hit-asia-hard

World Weather Attribution. (2024). Climate change made the deadly heatwaves that hit millions of highly vulnerable people across Asia more frequent and extreme. Retrieved from https://www.worldweatherattribution.org/climate-change-made-the-deadly-heatwaves-that-hit-millions-of-highly-vulnerable-people-across-asia-more-frequent-and-extreme/

XIE W., WANG Shuangshuang, YAN Xiaodong. 2022. Evaluation on CMIP6 Global Climate Model Simulation of the Annual Mean Daily Maximum and Minimum Air Temperature in China [J]. Climatic and Environmental Research (in Chinese), 27 (1): 63−78. DOI: 10.3878/j.issn.1006-9585.2021.21027

Xu, Z., Han, Y., Tam, CY. et al. Bias-corrected CMIP6 global dataset for dynamical downscaling of the historical and future climate (1979–2100). Sci Data 8, 293 (2021). https://doi.org/10.1038/s41597-021-01079-3

Yang, J., & Santamouris, M. (2018). Urban Heat Island and Mitigation Technologies in Asian and Australian Cities—Impact and Mitigation. *Urban Science*, *2*(3), 74. https://doi.org/10.3390/urbansci2030074

Yang, X., Zhou, B., Xu, Y. et al. CMIP6 Evaluation and Projection of Temperature and Precipitation over China. Adv. Atmos. Sci. 38, 817–830 (2021). https://doi.org/10.1007/s00376-021-0351-4

Yang, N., Lu, C., Ouyang, L. *et al.* Exploring spatial–temporal evolution patterns of urban heat islands in summer and winter: evidence from a megacity of China. *Sci Rep* **15**, 13592 (2025). https://doi.org/10.1038/s41598-025-97284-w

Yiou, P., Robert Vautard, Yoann Robin, Nathalie de Noblet-Ducoudré, Fabio D'Andrea, Robin Noyelle, How could 50 °C be reached in Paris: Analyzing the CMIP6 ensemble to design storylines for adaptation, Climate Services, Volume 36, 2024, 100518, ISSN 2405-8807, https://doi.org/10.1016/j.cliser.2024.100518.

Yuan, H., Ning, L., Zhou, J. et al. HiCPC: A new 10-km CMIP6 downscaled daily climate projections over China. Sci Data 11, 1167 (2024). https://doi.org/10.1038/s41597-024-03982-x

Zelinka, M. D., Myers, T. A., McCoy, D. T., Po-Chedley, S., Caldwell, P. M., Ceppi, P., ... & Taylor, K. E. (2020). Causes of higher climate sensitivity in CMIP6 models. *Geophysical Research Letters*, 47(1), e2019GL085782. https://doi.org/10.1029/2019GL085782

Zhao, L., Lee, X., Smith, R. B., & Oleson, K. (2014). Strong contributions of local background climate to urban heat islands. *Nature*, 511(7508), 216-219. https://doi.org/10.1038/nature13462

Zhao, L., Oleson, K., Bou-Zeid, E., Krayenhoff, E. S., Bray, A., Zhu, Q., ... & Oppenheimer, M. (2021). Global multi-model projections of local urban climates. *Nature Climate Change*, 11(2), 152-157. https://www.nature.com/articles/s41558-020-00958-8

Zhang, X., Lijuan Hua, Dabang Jiang, Assessment of CMIP6 model performance for temperature and precipitation in Xinjiang, China, Atmospheric and Oceanic Science Letters, Volume 15, Issue 2, 2022, 100128, ISSN 1674-2834, https://doi.org/10.1016/j.aosl.2021.100128.

Zhang, J., Wu, T., Li, L. *et al.* Constraint on regional land surface air temperature projections in CMIP6 multi-model ensemble. *npj Clim Atmos Sci* **6**, 85 (2023). https://doi.org/10.1038/s41612-023-00410-6

Zhang, C., Wu, G. & Zhao, R. Changes in the annual cycle of surface air temperature over China in the 21st century simulated by CMIP6 models. Sci Rep 15, 13661 (2025). https://doi.org/10.1038/s41598-025-98672-y

Zhong, X., T. Zhang, S. Kang, and J. Wang, 2022: Snow Depth Trends from CMIP6 Models Conflict with Observational Evidence. *J. Climate*, **35**, 1293–1307, https://doi.org/10.1175/JCLI-D-21-0177.1.

Zhu, Y., Saini Yang, Evaluation of CMIP6 for historical temperature and precipitation over the Tibetan Plateau and its comparison with CMIP5, Advances in Climate Change Research, Volume 11, Issue 3, 2020, Pages 239-251, ISSN 1674-9278, https://doi.org/10.1016/j.accre.2020.08.001.